Polyhedron 30 (2011) 2856–2862

Contents lists available at SciVerse ScienceDirect

Polyhedron

journal homepage: www.elsevier.com/locate/poly

Syntheses and structures of zinc and tin(II) compounds with hemilabile *N*-silyl-*tert*-butylamido and *N*-silyl-*p*-tolylamido ligands that contain pendent *tert*-butoxy groups

Gregory L. Fondong [a], Edmond Y. Njua [a], Alexander Steiner [b], Charles F. Campana [c], Lothar Stahl [a,*]

[a] Department of Chemistry, University of North Dakota, Grand Forks, ND 58202, USA
[b] Department of Chemistry, Crown Street, University of Liverpool, Liverpool L69 7ZD, UK
[c] Bruker AXS Inc., Madison, WI 53711, USA

ARTICLE INFO

Article history:
Received 24 March 2011
Accepted 10 August 2011
Available online 25 August 2011

Keywords:
(*N-tert*-butoxydimethylsilyl)-*tert*-butylamide
(*N-tert*-butoxydimethylsilyl)-*p*-tolylamide
N,O-donor ligands
N-silyl-amides
Hemilabile ligands
Zinc(II) amides
Tin(II) amides

ABSTRACT

Syntheses and solid-state structures of zinc and tin(II) compounds, containing the *N*-silyl-amide ligands (O^tBu)(NR)$SiMe_2$, R = ^{t}Bu (L^{tBu}), or R = *p*-tolyl (L^{pTol}), are reported. The *N*-silyl amines were synthesized by modified published procedures from commercially available Me_2SiCl_2, ^{t}BuOH, and ^{t}BuNH$_2$, or *p*-Me-$C_6H_4NH_2$, respectively. Treatment of $SnCl_2$ with LiL^{pTol} furnished $Sn(L^{pTol})_2$, which was X-ray structurally characterized and shown to contain two covalent Sn–N bonds and two asymmetrical O → Sn donor bonds. The single-crystal X-ray structure of $Sn(L^{tBu})_2$ revealed a much more symmetrically-coordinated, pseudo-trigonal-bipyramidal tin atom. Aminolysis of diethylzinc with HL^{pTol} produced $[EtZn(L^{pTol})]_2$, which crystallized as a centrosymmetric dimer, containing four-coordinate zinc atoms connected by bridging amides. Zinc dichloride, by contrast, reacted with two equivalents of LiL^{tBu} to produce the homoleptic, pseudo-spirocyclic $Zn(L^{tBu})_2$.

1. Introduction

Secondary amides are versatile ligands for main-group and transition metals, whose perhaps best known representative is the bis(trimethylsilyl)-substituted analog $N(SiMe_3)_2$, **A**, shown in Chart 1 [1,2]. Metal complexes of this ligand and its variants were first reported almost half a century ago [3], but now representatives for virtually all main-group [4–14] and transition [15–19] metals are known. It was suggested relatively early in the research on bulky, secondary amides that these molecules can be considered steric equivalents of cyclopentadienide, which in turn led to their widespread acceptance among organometallic chemists. The more recent success of amides of the type NRAr (Ar = 3,5-$C_6H_3Me_2$, R = ^{t}Bu, Me), **B**, as stabilizing ligands for early transition metals that are useful in the activation of small molecules renewed interest in the coordination chemistry of these *N*-donor ligands [20–22]. Among the most popular main group derivatives of **A** is the heterocarbenoid $Sn[N(SiMe_3)_2]_2$, **C**, which was first reported by Lappert and co-workers [23–27]. The diverse reactivity patterns and reaction products of this stannylene have made it popular among main group and transition metal chemists alike.

We are studying insertions of **C** and its germanium analog into the P–Cl bonds of chlorophosphines. Because these reactions are often too fast to be followed by conventional NMR techniques, we tried to attenuate the reactivity of the carbenoids by using amides with intramolecular donor groups. For reasons of synthetic utility we chose *tert*-butyl- and *p*-tolyl-amide-based ligands of the type (O^tBu)(NR)$SiMe_2$, **D**, because they can be prepared from inexpensive dichlorodimethylsilane and the appropriate amine and *tert*-butanol. The main-group chemistry of (O^tBu)(HN^tBu)$SiMe_2$ had been systematically investigated by Veith et al. [28–32]. Later Teuben and co-workers [33,34] and Edelmann and co-workers [35] described yttrium and lanthanide complexes, respectively, of this ligand.

In addition to ease of synthesis and chelating ability, one of the greatest assets of **D** is its modular nature, which makes it well suited for reactivity studies that probe both electronic and steric substituent effects. Below we report on syntheses and solid-state structures of *N*-(*tert*-butoxydimethylsilyl)-*tert*-butylamido and *N*-(*tert*-butoxydimethylsilyl)-*p*-tolylamido derivatives of tin(II). To better understand the ligand effects in the absence of lone-pair electrons, we also synthesized and X-ray structurally characterized their mono- and di-substituted zinc complexes.

* Corresponding author. Tel.: +1 701 777 2242; fax: +1 701 777 2331.
E-mail address: lstahl@chem.und.edu (L. Stahl).

0277-5387/$ - see front matter © 2011 Elsevier Ltd. All rights reserved.
doi:10.1016/j.poly.2011.08.011

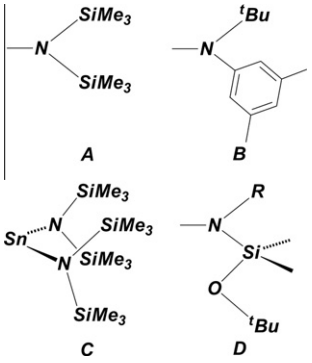

Chart 1. Selected secondary amides and a tin(II) derivative of $N(SiMe_3)_2$.

2. Results and discussion

The syntheses of all ligands reported herein are based on the intermediate chloro/*tert*-butoxydimethylsilane, **1**, which was prepared from dichlorodimethylsilane. We encountered problems in the selective mono-alkoxylation of the dichlorodimethylsilane with NaO^tBu, as described in the original report [28], often obtaining di-*tert*-butoxydimethylsilane that was difficult to separate from the chloro-*tert*-butoxydimethylsilane. This may be related to the quality of the commercial NaO^tBu, whose purity is difficult to assess. In our hands the synthesis of **1** via the addition of one equivalent of *tert*-butanol to dichlorodimethylsilane in the presence of pyridine (Scheme 1) proved superior, as it gave consistently only the desired mono-*tert*-butoxydimethylsilane. Removal of the pyridinium chloride by filtration and vacuum distillation (38 °C, 5 torr) of the filtrate afforded **1** in ca. 50% yield.

The *N*-silyl-*tert*-butylamine $(O^tBu)(NH^tBu)SiMe_2$, **2**, was synthesized according to a published procedure from **1** and two equivalents of *tert*-butylamine [28]. For the *p*-toluidine-based ligand, we chose the modified procedure shown in Scheme 2. Removal of lithium chloride by filtration, followed by vacuum distillation of the residue furnished $(O^tBu)(NH\text{-}4\text{-}C_6H_4Me)SiMe_2$, **3**, in 82% yield.

Using a slightly modified literature method [29], the bis[(*tert*-butoxydimethylsilyl)amide]tin compounds **4** and **5** were synthesized as shown in Scheme 3 and isolated as crystalline, light-yellow solids in good yields. Compound **4** was previously reported to have a melting point of 40 °C [29], which may have precluded a single-crystal X-ray analysis. The crystals we isolated melted at ca. 60 °C; they were thus easier to manipulate and subjected to a single-crystal X-ray study. Crystal and refinement parameters for **4** are listed in Table 1, while selected bond parameters are given in the caption of Fig. 1.

The compound crystallizes with two independent molecules in the monoclinic unit cell, space group $P2_1/n$, of which one, **4a**, is shown in Fig. 1. As can be seen in the thermal ellipsoid plot, the molecule is a pseudo-spirocycle in which the central tin(II) atom is chelated by both *N,O* ligands. Although the lone pair of electrons

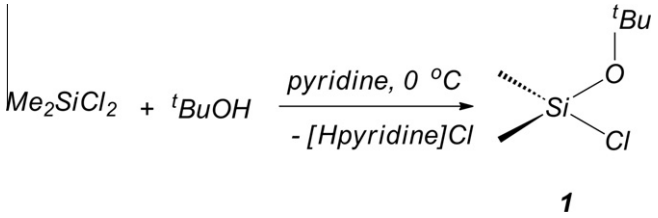

Scheme 1. Synthesis of **1**.

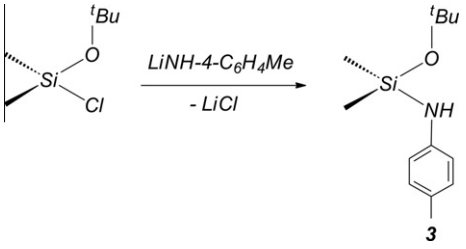

Scheme 2. Synthesis of **3**.

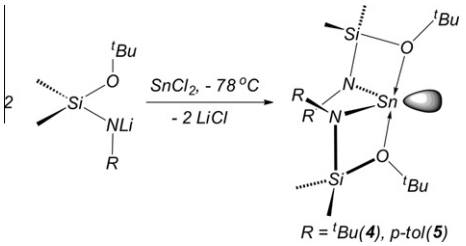

Scheme 3. Syntheses of **4** and **5**.

is clearly stereochemically active the bond angels about the tin atom correspond to neither tetrahedral nor to trigonal-bipyramidal (tbp) geometry. Thus, while the O–Sn–O angle is essentially linear (177.16(4)°), as would be expected for a tbp structure, the N–Sn–N angle spans only 101.68(6)° and is thus closer to the value expected for tetrahedral geometry. For comparison, the N–Sn–N angle in **C** is only slightly larger at 104.7(2)°. As is typical for spirocycles, the N–Sn–O angles are extremely acute. In **4a**, however, the angle compression is even more severe, with values of 63.11(5)° and 63.27(4)°, respectively, because the O → Sn donor-bonds are not subject to the same angle strain as covalent bonds. At 2.1548(16) and 2.1486(16) Å the almost symmetrical tin–nitrogen bonds are elongated compared to those in **C**, where they are ca. 2.09 Å long [27]. The equidistant O···Sn contacts (Sn1–O1 = 2.6184(14) and Sn1–O2 = 2.6240(14) Å) are much longer than covalent Sn–O bonds (1.995–2.071 Å) [36–39], but significantly shorter than the sum of the van der Waals radii of these elements (3.69 Å) [40,41].

The second independent molecule, **4b**, is shown in Fig. 2 in a perspective that emphasizes its close structural relationship to stannylene **C**. In essence, **4b** is an analog of Lappert's stannylene with two additional O → Sn donor interactions, which may compromise the carbenoid nature of the molecule. A comparison of the metric parameters, listed in the captions of Figs. 1 and 2, reveals the isostructural natures of **4a** and **4b**.

The *p*-tolyl-substituted analog of **4**, namely $Sn[(O^tBu)(N\text{-}4\text{-}C_6H_4Me)SiMe_2]_2$ (**5**), crystallizes in the monoclinic system, space group $P2_1/n$, but with the conventional four molecules in the unit cell. Crystal and refinement data for **5** are collected in Table 1, and the caption of Fig. 3 contains selected bond parameters. As the thermal-ellipsoid plot shows, the solid-state structure of this compound is noticeably less symmetrical than that of **4**. Thus, the N1, O1 ligand chelates the tin atom in a manner similar to that in **4**, with a comparable Sn–N bond of 2.1438(19) Å, but a shorter O → Sn donor bond 2.3753(17) Å. The tin–nitrogen bond (Sn–N2) of the second ligand is similarly short (2.095(2) Å) as those in **C**, but it is accompanied by a much longer Sn···O contact (2.97(3) Å). Conventional O → Sn donor bonds in complexes like $SnClBr(THF)_2$ [42], for example, are ca. 2.40–2.50 Å long; separations approaching 3 Å thus fall well outside of the range of donor bonds between these elements. It is therefore better to view the tin atom in this molecule as three coordinate. It

Table 1
Crystal, data collection, and refinement parameters for **4**–**7**.

Compound	**4**	**5**	**6**	**7**
Molecular formula	$C_{20}H_{48}N_2O_2Si_2Sn$	$C_{26}H_{44}N_2O_2Si_2Sn$	$C_{30}H_{54}N_2O_2Si_2Zn_2$	$C_{20}H_{48}N_2O_2Si_2Zn$
Formula weight	523.47	591.50	661.68	470.15
Space group (no.)	$P2_1/n$(14)	$P2_1/n$(14)	$P\bar{1}$(2)	$P2_1/c$(14)
T (K)	173	173	173	173
a (Å)	16.7929(16)	9.0822(17)	10.9560(15)	18.3798(18)
b (Å)	11.9038(11)	15.450(3)	12.8020(17)	18.1299(18)
c (Å)	28.263(3)	22.607(4)	12.9093(18)	18.4131(18)
α (°)			89.575(2)	
β (°)	98.777(2)	99.040(3)	87.730(2)	112.321(3)
γ (°)			74.677(2)	
V (Å^3)	5583.7(9)	3132.9(10)	1744.9(4)	5675.9(10)
Z	8	4	2	8
λ (Å)	0.71073	0.71073	0.71073	0.71073
ρ_{calc} g cm^{-3}	1.245	1.254	1.259	1.100
μ (mm^{-1})	1.016	0.914	1.470	0.965
F(000)	2208	1232	704	2048
θ Range (°)	1.86–28.26	1.60–28.32	1.58–27.50	1.12–22.26
Data/restraints/parameters	12909/0/519	7271/68/360	7638/0/357	7323/416/539
Goodness-of-fit (GOF) on F^2	1.028	1.067	1.048	1.053
$R(F)$[a] [$I > 2\sigma(I)$]	0.0277	0.0343	0.0375	0.0758
wR_2 (F^2)[b] [all data]	0.0727	0.0895	0.1039	0.2094
Largest difference in peak and hole (e Å^{-3})	1.197, −0.294	1.103, −0.235	0.772, −0.258	1.599, −0.370

[a] $R = \Sigma||F_o| - |F_c||/\Sigma|F_o|$.
[b] $wR_2 = \{[\Sigma w(F_o^2 - F_c^2)]/[\Sigma w(F_o^2)^2]\}^{1/2}$; $w = 1/[\sigma^2(F_o)^2 + (xP)^2 + yP]$ where $P = (\text{Maximum } (F_o^2 + 0) + 2F_c^2)/3$.

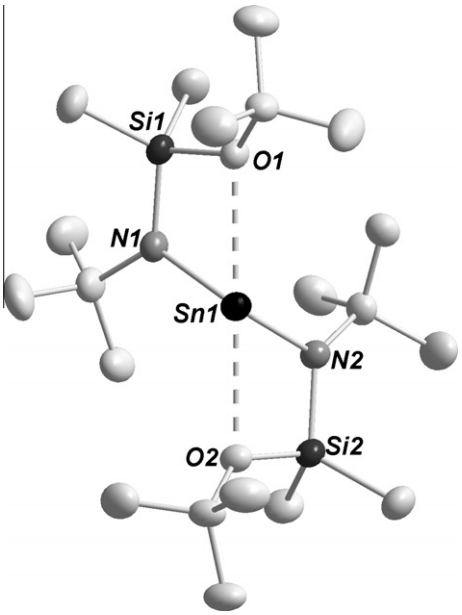

Fig. 1. Solid-state structure of **4a**, emphasizing the pseudo trigonal-bipyramidal structure of the compound. All atoms are drawn as 50% thermal ellipsoids and hydrogen atoms have been omitted for clarity. Selected bond lengths (Å) and angles (°): Sn1–N1 2.1545(16); Sn1–N2 2.1488(16); Sn1–O1 2.6184(14); Sn1–O2 2.6240(14); N1–Sn1–N2 101.68(6); O1–Sn1–O2 177.16(4); O1–Sn1–N1 63.27(4); O1–Sn1–N2 115.24(5); O2–Sn1–N2 63.11(5); O2–Sn1–N1 114.44(5).

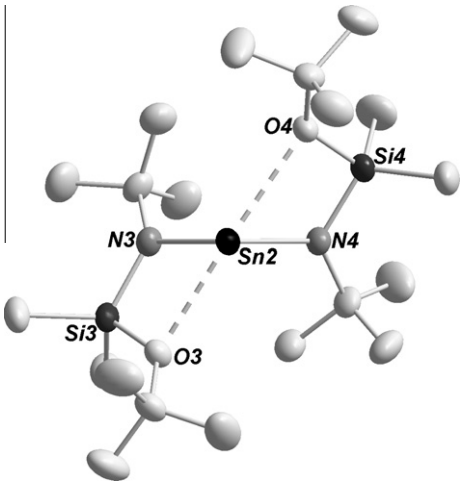

Fig. 2. Solid-state structure and partial labeling scheme of **4b**, in a perspective that emphasizes its relationship to **C**. All atoms are drawn as 50% thermal ellipsoids and hydrogen atoms have been omitted for clarity. Selected bond lengths (Å) and angles (°): Sn2–N3 2.1406(16); Sn2–N4 2.1479(16); Sn2–O3 2.5970(13); Sn2–O4 2.6829(14); N3–Sn2–N4 101.89(7); O3–Sn2–O4 174.81(4); O3–Sn2–N3 63.31(5); O3–Sn2–N4 112.55(5); O4–Sn2–N4 62.57(5); O4–Sn2–N3 115.09(5).

may be noted that the *p*-tolyl groups in both ligands of this compound have decidedly different conformations, the aromatic ring in ligand 1 (N1 and O1) being coplanar with the heterocycle, while that in ligand 2 (N2 and O2) is perpendicular to it. Whether these conformational differences reflect real effects – be they inductive or resonance – exerted by the aryl groups or whether they are merely packing artifacts is not clear. The asymmetry of **5** is also reflected in the bond angles, which at least in some cases differ significantly from those of **4a** and **4b**. For example, the N(1)–Sn(1)–N(2) angle is only 95.19(7)° and thus substantially more acute than in the *tert*-butylamido based ligand; this may be due to the lesser steric demands of the *p*-tolyl substituents.

As expected, there is no evidence for this asymmetry in the room temperature, solution-phase ^{1}H NMR spectrum of **5**, which consists of two doublets in the aromatic region at 6.51 and 6.84 ppm, and three singlets in the aliphatic region at 2.17, 1.36, and 0.050 ppm, the latter signals being assigned to the *p*-methyl, *tert*-butyl, and trimethylsilyl groups, respectively. The ^{1}H NMR spectrum of **4** exhibits singlets at δ = 1.37, 1.34, and 0.31 ppm for the *O-tert*-butyl, *N-tert*-butyl, and equivalent silyl methyl groups, respectively. This, too, suggests fluxional ligands, because in the solid the MeSi groups are diastereotopic and therefore should yield two signals if this conformation were maintained in solution.

Because of the obvious stereochemical activity of the lone pair of electrons in **4** and **5** we chose to obtain structural information on zinc complexes which are free of this complicating feature. Zinc

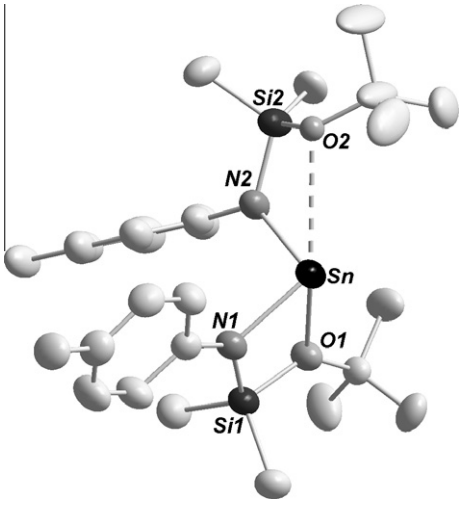

Fig. 3. Thermal ellipsoid plot and partial labeling scheme of **5**. All but the carbon atoms (35%) are drawn as 50% ellipsoids. Selected bond lengths (Å) and angles (°): Sn–N1 2.1438(19); Sn–N2 2.095(2); Sn–O1 2.3753(17); Sn–O2 2.97(3); N1–Sn–N2 95.19(7); O1–Sn–O2 144.1(5); O1–Sn–N1 92.56(9); O1–Sn–N2 94.02(7); O2–Sn–N2 56.1(5); O2–Sn–N1 130.1(6).

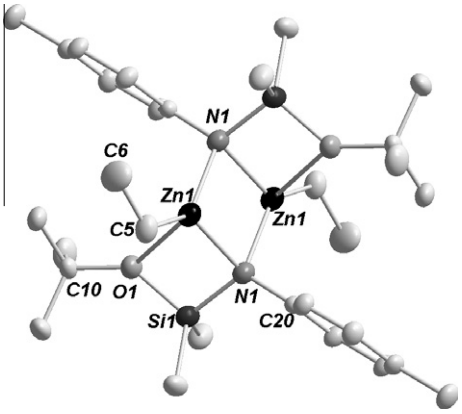

Fig. 4. Thermal-ellipsoid plot and partial labeling scheme of one (**6a**) of the two dimers of **6**. All but the carbon atoms (35%) are drawn as 50% ellipsoids. Selected bond lengths (Å) and angles (°): Zn1–N1 2.1019(19); Zn1–N1′ 2.057(2); Zn1–O1 2.4446(18); Zn1–C5 1.976(3); N1–Zn1–N1′ 91.57(7); Zn1–N1–Zn1′ 88.43(7); N1–Zn1–O1 67.93(7); N1–Zn1–C5 130.40(11); O1–Zn1–C5 106.19(10); O1–Si1–N1 97.69(9).

has an extensive chemistry involving primary and secondary amides, with both hydrocarbyl and silyl substituents [43–46]. Although some of these show zinc in a linear, two-coordinate environment, three- and four-coordinate zinc complexes are far more common, particularly in those cases where the ligands have additional donor sites. Divalent zinc with its closed-shell d^{10} configuration is somewhat similar to tin(II), but zinc is more Lewis acidic and with a covalent radius of 1.25 Å also significantly smaller than the Group 14 metal. The attempted synthesis of Zn[(O^{t}Bu)(N-4-C_6H_4Me)$SiMe_2$]$_2$ via the aminolysis of $ZnEt_2$ with one or two equivalents of HL^{pTol}, even on prolonged refluxing, invariably gave only the mono-ligand derivative **6**, shown in Scheme 4.

The colorless compound crystallizes in the triclinic space group $P\bar{1}$, with two crystallographically-independent dimers in the unit cell. Crystal data and refinement parameters for **6a** are listed in Table 1, while selected bond parameters are provided in the caption of Fig. 4. The second dimer has virtually identical bond parameters, which may be accessed in the supplementary crystallographic data.

As Fig. 4 shows, the compound has a ladder-type structure, so commonly found for main-group metal compounds. Such dimeric, or oligomeric, ladders are often the result of intermolecular Lewis acid–base interactions. At first glance **6a** appears to be of this type, consisting of dimers of EtZnL^{pTol} moieties in which the nitrogen atom of one unit is connected to the zinc atom of the opposing unit via a donor bond. Closer inspection, however, reveals that the putative N → Zn donor bond is actually shorter than the "intramolecular" bond, the former being 2.058(2) Å long, while the latter is 2.1026(18) Å in length. This confirms that **6a** is really a dinuclear complex in which the secondary amides bridge two zinc centers in a slightly asymmetrical fashion. Because of this bridging interaction both zinc–nitrogen bonds are substantially longer than those in two-coordinate complexes, like Zn[N(SiMe$_3$)$_2$]$_2$, where they are merely 1.833(11) Å long [47]. For comparison, in the methyl-zinc guanidinate monomer Zn[Me$_2$NC(N^{i}Pr)$_2$]OBMes$_2$ the Zn–N bonds are 2.0287(17) and 2.0645(16) Å long, while they measure 2.063(3) and 2.101(3) Å, respectively, in the related dimer {[MeZn(-N^{i}Pr)$_2$CN(SiMe$_3$)$_2$]}$_2$ [48,49]. The coordination environments of the zinc centers in **6a** are completed by normal-length zinc–ethyl bonds (1.975(3) Å) and O → Zn donor bonds (2.4447(17) Å), which are comparatively shorter than those in the tin compounds **4** and **5**. To a first approximation the zinc atoms are tetrahedrally coordinated, but because of their inclusion in a polycyclic structure the bond angles naturally differ from tetrahedral values.

The failure of $ZnEt_2$ to furnish diligated zinc derivatives served as a reminder that such species are better accessed via zinc diamides, like Zn[N(SiMe$_3$)$_2$]$_2$ [49], or by treating zinc chloride with alkali metal amides [50,51]. To obtain a monomeric zinc compound with two of the title ligands we treated anhydrous zinc chloride with two equivalents of the lithium salt of **2** in hexanes, as shown in Scheme 5. The reaction proceeded cleanly and furnished colorless **7** in high yield. The simple ^{1}H NMR spectra, revealing only two sharp singlets for the chemically-inequivalent *tert*-butyl groups and one singlet for the $SiMe_2$ groups, were consistent with a symmetrical molecule. The compound proved to be exceedingly soluble even in hexanes, suggesting a monomeric compound free of intermolecular O···Zn interactions. A single-crystal X-ray analysis confirmed this assumption, and Fig. 5 shows the solid-state structure of **7**, which crystallizes in the monoclinic space group $P2_1/c$ with two crystallographically-independent molecules. In both molecules the zinc atom and one of the ligands are

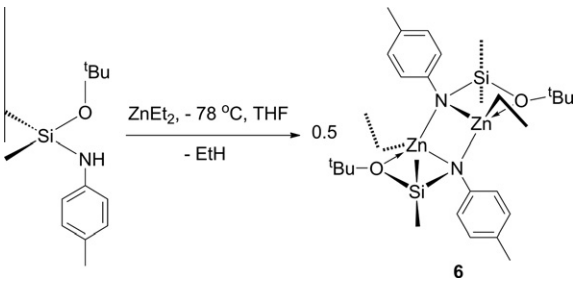

Scheme 4. Synthesis of **6**.

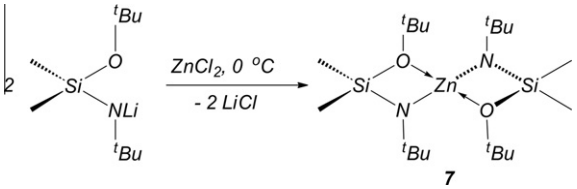

Scheme 5. Synthesis of **7**.

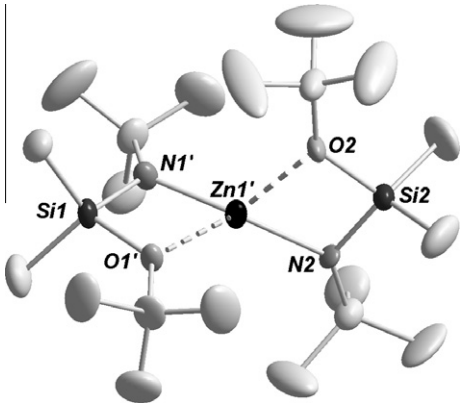

Fig. 5. Thermal-ellipsoid plot and partial labeling scheme of one (**7a**) of the independent molecules of **7**. For clarity hydrogen atoms have been omitted; all but the carbon atoms (30%) are drawn as 50% ellipsoids. Selected bond lengths (Å) and angles (°): Zn1–N1 1.879(5); Zn1–N2 1.840(5); Zn1–O1 2.381(7); Zn1–O2 2.352(5); N1–Zn1–N2 164.0(4); O1–Zn1–O2 100.3(3); N1–Zn1–O1 70.8(2); N1–Zn1–O2 117.9(2); N2–Zn1–O1 122.3(4); N2–Zn1–O2 71.1(2); N1–Si1–O1 95.9(2); N2–Si2–O2 95.6(2).

disordered; the latter in such a manner that the nitrogen and oxygen atoms and their respective *tert*-butyl groups share sites. Fig. 5 shows one of these molecules, **7a**, but with the disorder removed and only one of two positions of the zinc atom and of the disordered ligand shown.

Although **7** appears to be a spirocycle with an almost tetrahedrally-coordinated zinc atom, the bond lengths and angles suggest that the metal is better viewed as 2 + 2 coordinated, having two short (covalent) and two long (donor) bonds. Thus, the Zn–N bonds in **7** are barely longer than those in truly two-coordinate zinc amides, c.f., $Zn(N^tBu_2)_2$, with Zn–N = 1.824(3) and 1.831(3) Å [50], respectively, and $Zn[N(SiPh_2Me)_2]_2$ with an average Zn–N length of 1.850(3) Å [51]. A gas electron diffraction study on $Zn[N(SiMe_3)_2]_2$ revealed a linear molecule with symmetrical Zn–N bonds that are 1.824(14) Å long [47]. At 2.3198(6) and 2.3444(6) Å the O → Zn donor bonds in **7** are substantially shorter than those in dimeric **6** (2.4446(18) Å), but longer than those in ether adducts or related four-coordinate zinc compounds, where these bonds can be as short as 2.193(4) Å [52]. It is illustrative that the O → Zn donor bonds in **7** are almost equidistant with those in $Zn[(CH_2)_nOMe]_2$, $n = 3$, 4, where they are 2.37(3) and 2.38(5) Å long, respectively, suggestive of similar interactions [24]. In keeping with the bond-length trends, the N–Zn–N angle (164.0°) is much closer to linear than to tetrahedral. The zinc derivative **7** is a structural analog of $Mg[(O^tBu)(N^tBu)SiMe_2]_2$, which was reported as early as 1982 but whose solid-state structure was never determined [28]. Based on ^1H NMR evidence the authors proposed a spirocyclic molecule, and the structure of **7** supports this assignment.

The zinc complexes **6** and **7** were synthesized mainly to observe the ligand coordination in a divalent metal devoid of lone pair electrons. We mention parenthetically that zinc amide chemistry has seen enormous growth in the past decades [2], and that zinc amides with internal donor groups are being investigated, among others, as zinc source materials for vapor deposition techniques [53]. Contrary to our expectations monosubstitution of $ZnEt_2$ by L^{pTol} did not give monomeric $EtZnL^{pTol}$, but furnished instead the dinuclear $EtZn(\mu\text{-}L^{pTol})_2ZnEt$, which contains two bridging amido groups. In such dimers the zinc centers suffer greater steric congestion, thereby preventing the coordination of a second amine and the subsequent aminolysis of the remaining Zn–C bond. The solid-state structure of **6** Fig. 3, is remarkably similar to the ladder structure (**E**) of alkali metal derivatives of L^{tBu} and related ligands [30,31]. The failure of these alkali metal dimers of L^{tBu} to dissociate to monomers in solution upon addition of mono- and bidentate donor ligands, like THF, dioxane, and bipyridine, shows that bridging amides are present even in these ionic compounds.

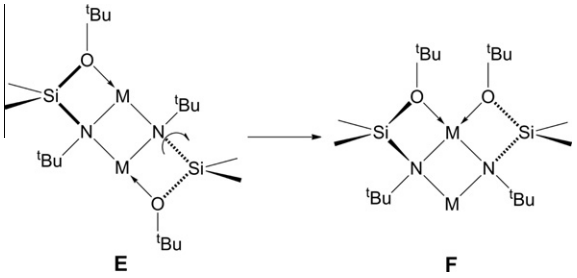

Scheme 6. Interconversion from ladder structure (**E**) to butterfly structure (**F**).

Conceptually, the ladder isomer **E** may be interconverted to the butterfly form **F** by the release of one O → M donor bond and the rotation of the "free" SiO^tBu group about an Si–N bond, as shown in Scheme 6. It is thus conceivable that **6** exhibits structure **F** in solution and structure **E** in the solid state, but no experimental evidence for such a rearrangement exists.

Based on the X-ray structural data, the title ligands are best considered bulky secondary amides with pendant alkoxy groups, in which the latter interact to a varying degree with the central metal atom. In the tin complexes this interaction is likely very weak in solution, because it barely exists in the solid state. The more Lewis-acidic zinc centers interact more strongly with the oxygen atoms, as reflected in their shorter O → M bonds.

3. Conclusion

The *tert*-butoxydimethylsilylamides $[(O^tBu)(NR)SiMe_2]^-$, R = ^{t}Bu, *p*-tolyl, are versatile hemilabile ligands that are characterized by ease of synthesis and coordinative flexibility, which is reflected in the solid-state structures of their tin(II) complexes. Thus, while L^{tBu} creates four-coordinate tin centers with pseudo trigonal-bipyramidal structures, the L^{pTol} ligands produces a three-coordinate metal center in which one ligand chelates the tin(II) ion while the second ligand is bound through its nitrogen atom only. This difference suggests weak O → Sn donor bonds, a feature which should aid in the utility of these ligands for Group 14 heterocarbenoids where such hemilability is desirable. The failure of diethylzinc to undergo complete aminolysis by $(O^tBu)(NHR)SiMe_2$ can be ascribed to the steric hindrance of the second Zn–C bond. Instead, two of these ligands bridge two metal centers to form a ladder-type structure in the solid state. A homoleptic $Zn(L^{tBu})_2$ complex, featuring a pseudo-tetrahedrally coordinated zinc ion, was obtained by treating $ZnCl_2$ with two equivalents of the LiL^{tBu}.

4. Experimental

4.1. General considerations

All experiments were performed under an atmosphere of purified nitrogen or argon, using standard Schlenk techniques. Dichloromethane was distilled from CaH_2 and stored over molecular sieves. THF was pre-dried with CaH_2 and like the hydrocarbon solvents dried and freed of molecular oxygen by distillation under an atmosphere of nitrogen from sodium or potassium benzophenone ketyl immediately before use. NMR spectra were recorded on a Bruker Avance 500 NMR spectrometer. The NMR spectra were referenced relative to benzene-d_6 (^1H = 7.15, ^{13}C = 128.0 ppm), THF-d_8 (^1H = 3.58 and 1.73 ppm, ^{13}C = 67.57 and 25.37 ppm) dichloromethane-d_2 (^1H = 5.32, ^{13}C = 54.00 ppm), respectively. Melting points were obtained on sealed samples with a Mel-Temp

apparatus; they are uncorrected. Midwest Micro Labs, LLC, Indianapolis, IN, and Desert Analytics, Tucson, AZ performed elemental analyses. The reagents Me_2SiCl_2 and $^tBuNH_2$ were purchased from Aldrich and distilled prior to use. *Tert*-butanol was obtained from Aldrich and stored over molecular sieves. Anhydrous $SnCl_2$ and $ZnCl_2$ were obtained from Strem, and $ZnEt_2$ was purchased from Aldrich; all were used as received. The $Me_2Si(^tBuO)(NH^tBu)$ was synthesized by a published method [28].

4.2. Syntheses

4.2.1. $Me_2(O^tBu)SiCl$ (**1**)

Dichlorodimethylsilane (67.0 mL, 0.550 mol), pyridine (45.3 mL, 0.560 mol), and THF (550 mL) were combined in a 2000 mL, three-necked flask, equipped with a magnetic stirbar. The mixture was chilled to 0 °C and treated dropwise with a solution of *tert*-butanol (52.6 mL, 550 mmol) in THF (50 mL), which produced a cloudy-white suspension that was allowed to stir at room temperature overnight. The reaction mixture was filtered on a medium-porosity frit and distilled (5 torr, 38 °C) using a Vigreux column to obtain analytically-pure **1** (by NMR) as a colorless oil. Yield: 46.2 g, 49%. The spectroscopic and physical properties of this compound were identical to those described in the literature [28].

4.2.2. $(O^tBu)(NH\text{-}4\text{-}C_6H_4Me)SiMe_2$ (**3**)

A 100 mL two-necked, round-bottom flask was charged with *p*-toluidine (2.67 g, 24.9 mmol) and hexanes (50 mL). The contents was cooled to 0 °C and treated dropwise with ^{n}BuLi (2.90 M in hexanes, 8.60 mL, 24.9 mmol), resulting in the formation of a white precipitate. The mixture was stirred at 0 °C for 3 h, allowed to warm to room temperature and then treated with a solution of **1** (4.20 g, 24.9 mmol) in hexanes (10 mL). It was further diluted with hexanes (20 mL), allowed to stir overnight and then filtered through a medium-porosity frit. Vacuum distillation on a Vigreux column furnished a viscous, yellow oil. Yield: 5.71 g, 82%. ^{1}H NMR (500.1 MHz, benzene-d_6, 27 °C): δ 6.93 (d, J_{HH} = 8.10 Hz, 2H, Ar), 6.68 (d, J_{HH} = 8.37 Hz, 2H, Ar), 3.26 (s, 1H, NH), 2.14 (s, 3H, *p*-Me), 1.22 (s, 9H, ^{t}Bu), 0.19 (s, 6H, Me). $^{13}C\{^1H\}$NMR (125.8 MHz, benzene-d_6, 27 °C): δ 144.84 (s, *i*-Ar), 130.32 (s, *o*-Ar), 127.40 (s, *p*-Ar), 117.55 (s, *m*-Ar), 73.33 (s, $OC(CH_3)_3$), 32.25 (s, $OC(CH_3)_3$), 20.99 (s, $SiMe_2$) 1.01 (s, *p*-Me). *Anal.* Calc. for $C_{13}H_{23}NOSi$: C, 65.77; H, 9.76; N, 5.90. Found: C, 65.61; H, 9.44; N, 5.72%.

4.2.3. $Sn[(O^tBu)(N^tBu)SiMe_2]_2$ (**4**)

A solution of $(^tBuO)(NH^tBu)SiMe_2$, **2** (4.28 g, 21.0 mmol) in cold (0 °C) hexanes (20 mL) was treated dropwise with a solution of ^{n}BuLi (2.90 M, 8.27 mL, 24.0 mmol) in hexanes (15 mL). The light-yellow mixture was refluxed for 3 h, allowed to cool to RT, and then added dropwise to a cold (−78 °C) $SnCl_2$ (2.00 g, 10.5 mmol) solution in THF (20 mL). The reaction mixture was stirred overnight while it warmed to room temperature. All liquids were removed *in vacuo*, the residue was extracted into hexanes, and the extract was filtered on a medium-porosity frit. The filtrate was concentrated *in vacuo* and stored at −21 °C for 10 days, to afford 5.33 g of light-yellow crystals. Yield: 97%. M.p.: 60–62 °C. ^{1}H NMR (500.1 MHz, THF-d_8, 27 °C): δ 1.37 ppm (s, 18H, O^tBu), 1.34 (s, 18H, N^tBu), 0.310 (s, 12H, CH_3); $^{13}C\{^1H\}$ NMR (125.8 MHz, THF-d_8, 27 °C) δ 73.6 ppm (s, $OC(CH_3)_3$), 52.6 (s, $NC(CH_3)_3$), 36.1 (s, $OC(CH_3)_3$), 30.8 (s, $NC(CH_3)_3$), 3.52 (s, $SiMe_2$). *Anal.* Calc. for $C_{20}H_{48}N_2O_2Si_2Sn$: C, 45.89; H, 9.24; N, 5.35. Found: C, 45.81; H, 9.44; N, 5.22%.

4.2.4. $Sn[(O^tBu)(N\text{-}4\text{-}C_6H_4Me)SiMe_2]_2$ (**5**)

The procedure follows the synthesis of **4** described above. A lithium amide solution was prepared by combining $(O^tBu)(NH\text{-}4\text{-}C_6H_4Me)SiMe_2$, **3** (2.78 g, 11.7 mmol) and ^{n}BuLi (2.90 M, 4.00 mL, 11.7 mmol). This solution was added dropwise to a solution of $SnCl_2$ (1.11 g, 5.85 mmol) in THF (10 mL). After 12 h of stirring the solvent was removed *in vacuo*, and the residue was extracted into hexanes. The extract was filtered on a medium-porosity frit, concentrated *in vacuo* and stored at −21 °C for 1 week. This afforded yellow, X-ray quality crystals in 80% yield. M.p.: 100–101 °C. ^{1}H NMR (500.1 MHz, THF-d_8, 27 °C): δ 6.80 (d, J_{HH} = 8.05 Hz, 4H, Ar), 6.51 (d, J_{HH} = 8.22 Hz, 4H, Ar), 2.17 (s, 6H, *p*-Me), 1.36 (s, 18H, ^{t}Bu), 0.05 (s, 12H, Me). $^{13}C\{^1H\}$NMR (125.8 MHz, THF-d_8, 27 °C): δ 148.92 (s, *ipso*-Ar), 129.59 (s, *o*-Ar), 128.31 (s, *p*-Ar), 125.17 (s, *m*-Ar), 75.16, (s, $OC(CH_3)_3$), 32.49 (s, $OC(CH_3)_3$), 20.87 (s, *p*-Me), 4.19 (s, $SiMe_2$). *Anal.* Calc. for $C_{26}H_{44}N_2O_2Si_2Sn$: C, 52.79; H, 7.50; N, 4.74. Found: C, 52.60; H, 7.27; N, 4.63%.

4.2.5. $\{EtZn[(O^tBu)(N\text{-}4\text{-}C_6H_4Me)SiMe_2]\}_2$ (**6**)

A cold (−78 °C) solution of $(O^tBu)(NH\text{-}4\text{-}C_6H_4Me)SiMe_2$, **3**, (1.85 g, 7.80 mmol) in THF (14 mL) was treated dropwise with a solution of diethylzinc (1.0 M, 7.80 mL, 7.8 mmol) in THF (10 mL). The reaction mixture was stirred at −78 °C for 1 h, allowed to warm to room temperature and then stirred overnight, during which time it became bright yellow. All solvents were removed *in vacuo*, and the residue was extracted into hexanes, filtered, and stored at −21 °C. After several days colorless, X-ray quality crystals formed. Yield: 1.9 g, 73%. M.p.: 156–160 °C. ^{1}H NMR (500.1 MHz, dichloromethane-d_2, 27 °C): δ 6.97 (d, J_{HH} = 8.20 Hz, 4H, Ar), 6.84 (d, J_{HH} = 8.20 Hz, 4H, Ar), 2.24 (s, 6H, *p*-Me), 1.35 (t, J_{HH} = 8.10 Hz, 6H, $-CH_3$), 0.86 (s, 18H, O^tBu), 0.41 (q, J_{HH} = 8.10 Hz, 4H, $ZnCH_2$), 0.15 (s, $SiMe_2$); $^{13}C\{^1H\}$ NMR (125.8 MHz, dichloromethane-d_2, 27 °C): δ 148.30 (s, *i*-Ar), 130.77 (s, *p*-Ar), 130.3 (s, *o*-Ar), 126.1 (s, *m*-Ar), 74.6 (s, $OC(CH_3)_3$), 31.3 (s, $OC(CH_3)_3$), 20.8 (s, $ZnCH_2-$), 13.2 (s, $-CH_3$), 3.22 (s, $SiMe_2$). *Anal.* Calc. for $C_{15}H_{27}NOSiZn$: C, 54.46; H, 8.23; N, 4.23. Found: C, 54.26; H, 7.91; N, 4.34%.

4.2.6. $Zn[(O^tBu)(N^tBu)SiMe_2]_2$ (**7**)

A slurry of $ZnCl_2$ (1.05 g, 7.66 mmol) in cold hexanes (−78 °C) was treated dropwise with a solution of $(O^tBu)(LiN^tBu)SiMe_2$, prepared from $(O^tBu)(NH^tBu)SiMe_2$ (3.11 g, 15.3 mmol) and ^{n}BuLi (2.5 M, 6.5 mL, 16.3 mmol), as described in the synthesis of **4**. The reaction mixture was allowed to stir overnight, filtered, concentrated, and stored at −21 °C for several days. This afforded a large crop of clear, colorless crystals. Yield: 2.98 g, 83%. M.p.: 130–133 °C. ^{1}H NMR (500.1 MHz, benzene-d_6, 27 °C): δ 1.405 (s, 9H, O^tBu), 1.322 (s, 9H, N^tBu), 0.353 (s, 6H, $SiMe_2$); $^{13}C\{^1H\}$ NMR (125.8 MHz, benzene-d_6, 27 °C): δ 74.03 (s, $OC(CH_3)_3$), 51.24 (s, $NC(CH_3)_3$), 37.85 (s, $OC(CH_3)_3$), 32.83 (s, $NC(CH_3)_3$), 7.21 (s, $SiMe_2$). *Anal.* Calc. for $C_{20}H_{48}N_2O_2Si_2Zn$: C, 51.09; H, 10.29; N, 5.96. Found: C, 50.81; H, 9.95; N, 6.07%.

4.3. X-ray crystallography

4.3.1. Compounds **4**–**7**

Suitable, single crystals were coated with Paratone oil, attached to Litholoop or Mitegen sample holders, and manually centered on the diffractometer in a stream of cold nitrogen. Reflection intensities were collected with a Bruker Apex CCD diffractometer, equipped with an Oxford Cryosystems 700 Series Cryostream cooler, operating at 173 K. Data were measured using ω scans of 0.3° per frame for 20 s until a complete hemisphere had been collected. Cell parameters were retrieved using SMART [53] software and refined with SAINT [54] on all observed reflections. Data were reduced with SAINT, which corrects for Lp and decay. Empirical absorption corrections were applied with SADABS [55]. The structures were solved by direct methods with the SHELXS-97 [56] program and

refined by full-matrix least squares methods on F^2 with SHELXL-97 [57], incorporated in SHELXTL-PC, Version 5.03 [58].

Acknowledgment

We thank the University of North Dakota for funds to purchase the Bruker Apex Diffractometer.

Appendix A. Supplementary data

CCDC 818111, 818112, 818113 and 818114 contain the supplementary crystallographic data for **4**–**7**. These data can be obtained free of charge via http://www.ccdc.cam.ac.uk/conts/retrieving.html, or from the Cambridge Crystallographic Data Centre, 12 Union Road, Cambridge CB2 1EZ, UK; fax: (+44) 1223-336-033; or e-mail: deposit@ccdc.cam.ac.uk.

References

[1] M.F. Lappert, P.P. Power, A.R. Sanger, R.C. Srivastava, Metal and Metalloid Amides, Horwood-Wiley, Chichester, 1980.
[2] M.F. Lappert, A. Protchenko, P.P. Power, A. Seeber, Metal Amide Chemistry, Wiley, Chichester, 2009.
[3] U. Wannagat, H. Bürger, Monatsh. Chem. 94 (1963) 761.
[4] U. Wannagat, H. Autzen, H. Kuckertz, H.-J. Wismar, Z. Anorg. Allgem. Chem. 394 (1972) 254.
[5] G.M. Sheldrick, W.S. Sheldrick, J. Chem. Soc. (A) (1969) 2279.
[6] H. Bürger, W. Sawodny, U. Wannagat, J. Organomet. Chem. 3 (1965) 113.
[7] M.A. Petrie, K. Ruhlandt-Senge, H. Hope, P.P. Power, Bull. Soc. Chim. Fr. 130 (1993) 851.
[8] P.J. Brothers, R.J. Wehmschulte, M.M. Olmstead, K. Ruhlandt-Senge, S.R. Parkin, P.P. Power, Organometallics (1994) 2792.
[9] W. Vargas, U. Englich, K. Ruhlandt-Senge, Inorg. Chem. 41 (2002) 5602.
[10] M. Gillette-Kunath, W. Teng, K. Ruhlandt-Senge, Inorg. Chem. 44 (2005) 4862.
[11] M. Westerhausen, J. Greuel, H.-D. Hausen, W. Schwarz, Z. Anorg. Allg. Chem. 622 (1996) 1295.
[12] D.J. Burkey, E.K. Alexander, T.P. Hanusa, Organometallics 13 (1994) 2773.
[13] K.T. Quisenberry, C.K. Gren, R.E. White, T.W. Hanusa, W.W. Brennessel, Organometallics 27 (2007) 4354.
[14] X. He, B.C. Noll, A. Beatty, R.E. Mulvey, K.W. Henderson, J. Am. Chem. Soc. 126 (2004) 7444.
[15] D.C. Bradley, M.B. Hursthouse, C.W. Newing, Chem. Commun. (1971) 411.
[16] D.C. Bradley, M.B. Hursthouse, P.F. Rodesiler, Chem. Commun. (1969) 14.
[17] D.C. Bradley, M.B. Hursthouse, R.J. Smallwood, A.J. Welch, Chem. Commun. (1972) 872.
[18] J.J. Ellison, P.P. Power, S.C. Shoner, J. Am. Chem. Soc. 111 (1989) 8044.
[19] S. Suh, D.M. Hoffman, Inorg. Chem. 35 (1996) 5015.
[20] C.E. Laplaza, C.C. Cummins, Science 268 (1995) 861.
[21] C.E. Laplaza, M.J.A. Johnson, J.C. Peters, A.L. Odom, E. Kim, C.C. Cummins, G.N. George, I.J. Pickering, J. Am. Chem. Soc. 118 (1996) 8623.
[22] C.E. Laplaza, W.M. Davis, C.C. Cummins, Organometallics 14 (1995) 577.
[23] D.H. Harris, M.F. Lappert, J. Chem. Soc., Chem. Commun. (1974) 895.
[24] J. Boersma, L. Fernholt, A. Haaland, Acta Chem. Scand. A38 (1984) 523.
[25] P.J. Davidson, D.H. Harris, M.F. Lappert, J. Chem. Soc., Dalton Trans. (1976) 2268.
[26] M.J.S. Gynane, D.H. Harris, M.F. Lappert, P.P. Power, P. Rivière, M. Rivière-Baudet, J. Chem. Soc., Dalton (1977) 2004.
[27] T. Fjeldberg, H. Hope, M.F. Lappert, P.P. Power, A.J. Thorne, Chem. Commun. (1983) 639.
[28] M. Veith, R. Rösler, J. Organomet. Chem. 229 (1982) 131.
[29] M. Veith, P. Hobein, R. Rösler, Z. Naturforsch. 44b (1989) 1067.
[30] M. Veith, J. Böhnlein, Chem. Ber. 122 (1989) 603.
[31] M. Veith, J. Böhnlein, V. Huch, Chem. Ber. 122 (1989) 841.
[32] M. Veith, A. Rammo, Z. Anorg. Allg. Chem. 627 (2001) 662.
[33] R. Duchateau, T. Tuinstra, E.A.C. Brussee, A. Meetsma, P.T. van Duijnen, J.H. Teuben, Organometallics 16 (1997) 3511.
[34] R. Duchateau, E.A.C. Brussee, A. Meetsma, J.H. Teuben, Organometallics 16 (1997) 5506.
[35] A. Recknagel, A. Steiner, S. Brooker, D. Stalke, F.T. Edelmann, J. Organomet. Chem. 415 (1991) 315.
[36] N.N. Zemlyansky, V.I. Borisova, G.M. Kuznetsova, V.N. Khrustalev, Y.A. Ustynyuk, M.S. Nechaev, V.V. Lunin, J. Barrau, G. Rima, Organometallics 22 (2003) 1675.
[37] S.A. Ionkin, J.W. Marshall, M.B. Fish, Organometallics 25 (2005) 4170.
[38] B. Cetinkaya, I. Gümrükçü, M.F. Lappert, L.J. Atwood, D.R. Rogers, J.M. Zaworotko, J. Am. Chem. Soc. 102 (1980) 2088.
[39] V.N. Khrustalev, M.Y. Antipin, N.N. Zemlyansky, V.I. Borisova, Y.A. Ustynyuk, V.V. Lunin, J. Barrau, G. Rima, J. Organomet. Chem. 689 (2004) 478.
[40] A. Bondi, J. Phys. Chem. 68 (1964) 441.
[41] A. Bondi, J. Phys. Chem. 70 (1966) 3006.
[42] C. Janiak, R. Weimann, F. Görlitz, Organometallics (1997) 4933.
[43] M. Westerhausen, T. Bollwein, A. Pfitzner, T. Nilges, H.-J. Deiseroth, Inorg. Chim. Acta 312 (2001) 239.
[44] M. Westerhausen, A.N. Kneifel, A. Kalisch, Angew. Chem., Int. Ed. 44 (2005) 96.
[45] M. Westerhausen, T. Bollwein, N. Makropoulos, T.M. Rotter, T. Habereder, M. Suter, H. Nöth, Eur. J. Inorg. Chem. (2001) 851.
[46] C. Koch, A. Malassa, C. Agthe, H. Görls, R. Biedermann, H. Krautscheid, M. Westerhausen, Z. Anorg. Allg. Chem. 633 (2007) 375.
[47] A. Haaland, K. Hedberg, P.P. Power, Inorg. Chem. 23 (1984) 1972.
[48] S.J. Birch, S.R. Boss, S.C. Cole, M.P. Coles, R. Haigh, P.B. Hitchcock, A.E.H. Wheatley, Dalton Trans. (2004) 3568.
[49] M.P. Coles, P.B. Hitchcock, Eur. J. Inorg. Chem. (2004) 2662.
[50] H. Schumann, J. Gottfriedsen, F. Girgsdies, Z. Anorg. Allg. Chem. 623 (1997) 1881.
[51] P.P. Power, K. Ruhlandt-Senge, S.C. Shoner, Inorg. Chem. 30 (1991) 5013.
[52] G.R. Lief, D.F. Moser, L. Stahl, R.J. Staples, J. Organomet. Chem. 689 (2004) 1110.
[53] B. Luo, B.E. Kucera, W.L. Gladfelter, Polyhedron 29 (2010) 2795.
[54] SMART V 4.043 Software for the CCD Detector System, Bruker Analytical X-ray Systems, Madison, WI, 1995.
[55] SAINT V 4.035 Software for the CCD Detector System, Bruker Analytical X-ray Systems, Madison, WI, 1995.
[56] SADABS program for absorption corrections using the Bruker CCD Detector System. Based on: R. Blessing, Acta Crystallogr., Part A 51 (1995) 33.
[57] G.M. Sheldrick, SHELXS-97, Program for the Solution of Crystal Structures, University of Göttingen, Germany, 1990.
[58] G.M. Sheldrick, SHELXL-97, Program for the Solution of Crystal Structures, University of Göttingen, Germany, 1997.